The experimental results most suitable for comparisons with theory are the measured radiation patterns in the horizontal $x-y$ plane. In that case the effect of the wedges of the cylinder may be shown to be negligible and we can study the distorting effect of the thin wire. Radiation patterns measured at a frequency of 10 GHz for $l = 7{\cdot}5$ mm and $H = 50$, 52 and 54 mm are shown in Fig. 2*a* with solid lines. In this geometry the theory of Reference 2 is inapplicable because it assumes a plane wave incident upon the wire. The K & A theory should, however, be applicable because the wire appears to be very long when viewed from the source point. The agreement is indeed remarkable as may be seen in Fig. 2*a*. For $l = 37{\cdot}5$ mm and $H = 50$ mm the agreement with the K & A theory is equally good but for shorter wire lengths the agreement deteriorates as may be seen in Fig. 2*b*. Using the theory of Reference 2 no improvement was obtained but we could improve the agreement by adding the tip-diffracted rays of Reference 2 to the scattered rays of the K & A theory. The construction is shown in Fig. 1*b*. The total scattered field is now made up of the K & A ray scattered at $P_1$ and the two rays (direct and reflected) scattered at the tip, $P_2$. The calculated radiation patterns are compared with the measured results in Figs. 2*c* and 2*d* for $H = 21$ mm and 25 mm, respectively. The agreement is good in both cases.

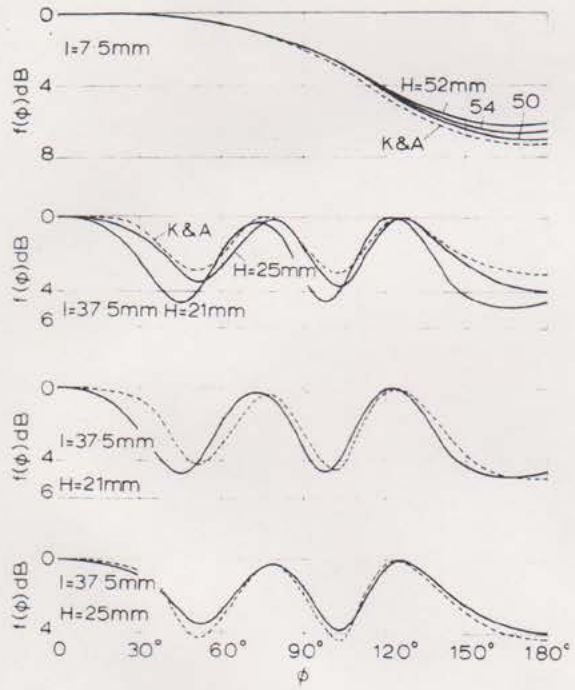


**Fig. 2**

——— measured
– – – – theoretical radiation patterns as functions of $\phi$ ($\phi = 0$ is the direction determined by the monopole and the wire)

For further experimental results for $l = 37{\cdot}5$ mm and for various wire lengths and wire diameters see the report of Albertsen *et al.*[3] All cases investigated bear out the above conclusions. The addition of tip-diffracted rays improves the agreement with the measured results.

Finally, we would like to note (for more details see Reference 3) that it is possible to derive a more rigorous formula for the diffraction coefficient than that given in Reference 2. It may be extracted from the theories of Vainshteyn[4] and Ufimtsev[5] leading to the form

$$D(\theta_1,\theta_2) = \left\{ -\frac{i}{2} \frac{\ln \dfrac{i}{\gamma ka \sin(\theta_1/2)\sin(\theta_2/2)}}{\ln \dfrac{2i}{\gamma ka \sin\theta_1} \ln \dfrac{2i}{\gamma ka \sin\theta_2}} \right\} \times \frac{\tan(\theta_1/2)\tan(\theta_2/2)}{\cos\theta_1 + \cos\theta_2}$$

where $\theta_1$ = angle of incidence (see Fig. 1*b*), $\theta_2$ = angle of scattering and $\gamma$ = Euler's constant.

For the cases investigated in the present study, the above diffraction coefficients gave practically identical results to those obtained from Reference 2. Note, however, that these new diffraction coefficients are not only more accurate but have the further merit of being independent of the length of the wire and depend on local variables only.

Part of this work was supported by ESA. The authors wish to thank N. E. Jensen, ESTEC, and H. Bach, Technical University of Denmark; for a number of interesting and critical discussions. The measurements were carried out at the Radio Anechoic Chamber, Technical University of Denmark.

L. SOLYMAR

*27th February 1976*

*Department of Engineering Science*
*Oxford University*
*Oxford, England*

K. PONTOPPIDAN

*Tiera A/S*
*Pilestraede 4,*
*DK-1112*
*Copenhagen K, Denmark*

**References**

1 KELLER, J. B., and AHLUWALIA, D. S.: 'Diffraction by a curved wire' *SIAM J. Appl. Math.*, 1971, **20**, pp. 390–405
2 SOLYMAR, L.: 'Derivation of diffraction coefficients for a thin wire of finite length', *Electron. Lett.*, 1973, **9**, p. 438
3 ALBERTSEN, N. C., BACH, H., BALLING, P., JENSEN, F., PONTOPPIDAN, K., SOLYMAR, L., and SORENSEN, O.: 'A study of radiation pattern prediction for high frequency satellite antennas', Technical Report R 145, Electromagnetics Institute, Technical University of Denmark, Lyngby, Denmark, Oct. 1975, pp. 1–176
4 VAINSHTEYN, L. A.: 'Current waves in a thin cylindrical conductor. III. Variational method and its application to the theory of ideal and impedance conductors', *Sov. Phys–Tech. Phys.*, 1961, **6**, pp. 30–33
5 UFIMTSEV, P. YA.: 'Diffraction of plane electromagnetic waves by a thin cylindrical conductor'. *Radio & Electron. Eng.*, 1962, **7**, pp. 241–249

## PULSE BROADENING IN MULTIMODE OPTICAL FIBRES WITH LARGE $\Delta n/n$: NUMERICAL RESULTS

*Indexing terms: Fibre optics, Optical waveguides*

The r.m.s. impulse response width of germania doped fibres having power-law profiles at the carrier wavelength is evaluated with the help of a numerical method and measured values of $dn/d\lambda$. For $\Delta n/n \approx 0{\cdot}02$, our result exceeds by more than one order of magnitude that obtained from an analytical formula based on the assumption that $n\,dn/d\lambda$ varies linearly with $n^2$. The optimum profiles are found to differ very significantly from power-law profiles. Our numerical technique is based on scalar-ray optics. It is applicable to any fibre having a large $V$-number and a smooth profile.

Multimode fibres having relatively large $\Delta \equiv \Delta n/n$ (e.g., $\Delta \gtrsim 0{\cdot}01$) are attractive because of their high coupling efficiency to l.e.d. sources and because of their small sensitivity to microbending loss. Even if long-life monomode injection lasers prove feasible, multimode fibres may remain more attractive than monomode fibres for long-distance high-capacity transmission because of easier cabling and splicing. Links using multimode fibres can easily be upgraded if long-life laser sources become available. Monomode fibres, in contradistinction, are restricted to laser sources.

One key question, however, is whether high data rates can be transmitted through multimode fibres having large $\Delta$. One of the best experimental values reported[1] for the r.m.s. impulse response width is $\sigma = 10\,000\,\Delta^2$ ns/km, for $\Delta = 0{\cdot}01$. On the other hand, Olshansky and Keck theory[2] indicates that the r.m.s. impulse response width does not exceed $150\Delta^2$ ns/km for a power-law profile

$$n^2(r)/n^2(0) = 1 - 2\Delta(r/a)^{2\kappa} \quad \ldots\ldots\ldots \quad (1)$$

and a suitable value of the exponent $\kappa$. If this theoretical result

were applicable to real fibres, gigabit/s rates would be possible for values of $\Delta$ as large as 0·02. However, Olshansky and Keck's theory implicitly assumes that $n\,dn/d\lambda$ varies linearly with $n^2$ as the dopant concentration varies. It is easy to see that when this condition is not fulfilled, power-law profiles do not remain power-law profiles at neighbouring wavelengths. In that case it is incorrect to calculate the group velocity by differentiating $n(r, \lambda)$ in eqn. 1 with respect to $\lambda$. Our measurements[3] show that $n\,dn/d\lambda$ is *not*, in fact, a linear function of $n^2$ (See Fig. 1). The purpose of the present letter is to assess the practical significance of this lack of linearity. This is done by comparing the analytical results in Reference 2 to exact numerical results. This comparison suggests that the formula given in Reference 2 is applicable only to fibres with very small values of $\Delta$, typically $\Delta \leq 0{\cdot}005$.

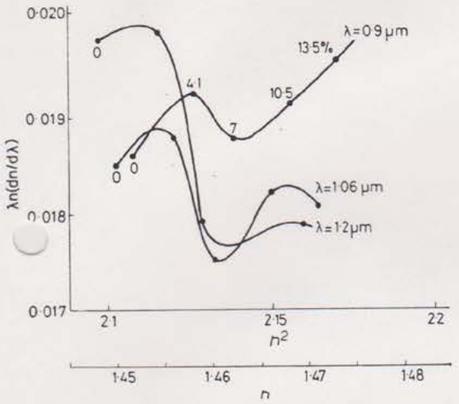


**Fig. 1** *Variation of $S \equiv -\lambda n(dn/d\lambda)$ for germania-doped fibres*

Measured with an accuracy of about 1%, as a function of $n^2$ at three wavelengths. The germania concentration in mole % is shown near the black dots. These curves exhibit large departures from linearity

The numerical technique presented in this letter is based on the space-time Hamilton equations.[4] All the information needed to write a working program is supplied but the detailed derivations are omitted. This technique gives accurately the r.m.s. impulse response width of dispersive fibres having large $V$-numbers ($V \gg 20$) and smooth profiles. About 1 minute of IBM 370 computer time is needed to evaluate the r.m.s. impulse response width of a fibre. This is one fifth of the time required by programs based on wave optics. For simplicity we assume that the source is quasimonochromatic (e.g., an l.e.d. followed by a narrow-band filter). The fibre response for sources with nonzero spectral width is easily obtained by convolving the quasimonochromatic response evaluated in this letter with the source spectrum.

Let us assume that the Sellmeier-law coefficients $A_\gamma$, $l_\gamma$, $\gamma = 1, 2$ and 3, of the materials incorporated in the fibre have been measured at the source wavelength. The refractive index $n$ is defined by the Sellmeier law

$$n^2 - 1 = \sum_{\gamma=1}^{3} A_\gamma (1 - \pi_\gamma)^{-1} \qquad \pi_\gamma = (l_\gamma/\lambda)^2 \quad . \quad (2)$$

We obtain by differentiation with respect to $\lambda$

$$S \equiv -\lambda n\, dn/d\lambda = \sum_{\gamma=1}^{3} A_\gamma \pi_\gamma (1 - \pi_\gamma)^{-2} \quad . \quad . \quad . \quad (3)$$

The variation of $S$ for germania-doped fibres is shown as a function of $n$ at three wavelengths of interest in Fig. 1. The measurements were made on prisms with 0, 4·1, 7, 10 and 13·5 mole % germania with the minimum deviation method. Note that angles of refraction, unlike optical thicknesses of thin samples, are insensitive to alterations of the sample surface that may be caused, for example, by oil films or compacting. Note also that the curves in Fig. 1 are independent of dopant concentration measurements. Quenching is found to affect only slightly the value of $dn/d\lambda$ at a constant $n$. Thus, the results are believed to be applicable to real fibres.

Let us now describe the ray sampling procedure. We select a normalised azimuthal mode number $M$ and a normalised propagation constant $B$ from the sequences

$$M = 1/A,\ \ 2/A, \ldots \quad . \quad . \quad . \quad . \quad . \quad . \quad . \quad . \quad . \quad (4a)$$

$$B = 2\Delta(I-1)/I,\ 2\Delta(I-2)/I, \ldots \quad . \quad . \quad . \quad . \quad . \quad . \quad (4b)$$

where $2\Delta \equiv 1 - n_c^2/n_o^2$, $n_o \equiv n(0)$, and $n_c$ is the cladding index. Typical values for $A$ and $I$ in eqn. 4 are 50 and 20, respectively.

The time of flight of a pulse along the ray trajectory specified by $M$ and $B$ is obtained by solving with the Euler or Runge–Kutta techniques the 1st-order equations

$$dR/dZ = (1-B)^{-1/2}\, P \quad . \quad . \quad . \quad . \quad . \quad . \quad . \quad . \quad . \quad (5a)$$

$$dP/dZ = (1-B)^{-1/2}(-\tfrac{1}{2}dN/dR + M^2/R^3) \quad . \quad . \quad (5b)$$

$$dT/dZ = (\bar{N}^2 - 2\bar{N} + B)/[1 - B + (1-\bar{N})(1-B)^{1/2}] \quad (5c)$$

for the three functions $R(Z)$, $P(Z)$ and $T(Z)$. We have defined a relative phase index $N$ and a relative group index $\bar{N}$ by

$$N(R) \equiv 1 - n^2(r)/n_o^2 \quad . \quad . \quad . \quad . \quad . \quad . \quad . \quad . \quad . \quad (6a)$$

$$\bar{N}(R) \equiv [N + (S_o - S)\, n_o^{-2}]/(1 + S_o\, n_o^{-2}) \quad . \quad . \quad . \quad (6b)$$

where $n$ and $S$ are defined in eqns. 2 and 3, respectively,

$$R \equiv r/a \qquad S_o \equiv S(0)$$

and $a$ denotes an arbitrary length, perhaps the core radius. (The fibre response is unaffected by a change of scale in the radial direction.) The initial values of $R(Z)$, $P(Z)$, $T(Z)$ are defined, respectively, by

$$R(0) = R_o \qquad dN(R_o)/dR_o = 2M^2/R_o^3 \quad . \quad . \quad . \quad (7a)$$

$$P(0) = [B - N(R_o) - M^2/R_o^2]^{1/2} \quad . \quad . \quad . \quad . \quad . \quad (7b)$$

$$T(0) = 0 \quad . \quad . \quad . \quad . \quad . \quad . \quad . \quad . \quad . \quad . \quad . \quad (7c)$$

The derivative $dN/dR$ in eqns 5*b* and 7*a* can be obtained algebraically if $N(R)$ is given as a simple analytical form such as a power-law profile, or by incrementing $R$. The integration of eqn. 5 terminates after one ray period. Usually, 2000 steps per period are sufficient. The difference between the time of arrival of a pulse along the ray considered and the time of arrival of a pulse along the fibre axis, in ns/km, is

$$\Delta t = 5000\, T_{final}/Z_{final} \quad . \quad . \quad . \quad . \quad . \quad . \quad . \quad . \quad (8)$$

The series of values of $M$ and $B$ taken in sequence according to eqn. 4 terminates when $P(0)$ in eqn. 7*b* ceases to be real. For a Lambertian source, the r.m.s. impulse response width $\sigma = (\langle \Delta t^2 \rangle - \langle \Delta t \rangle^2)^{1/2}$ is obtained by averaging $\Delta t$ in eqn. 8 over all the values of $M$ and $B$ permitted by the condition set up above. For non-Lambertian sources or nonuniform attenuation of the modes, one needs to introduce weighting factors in the evaluation of the averages.

The numerical technique just described has been applied to germania doped fibres that have the power-law profile in eqn. 1 at the source wavelength, but not necessarily at neighbouring wavelengths. We have considered two cases: A fibre with 10% germania on axis ($\Delta \approx 0{\cdot}011$) and a fibre with 20% germania on axis ($\Delta \approx 0{\cdot}22$). The cladding is assumed to be made of pure silica. The values for $S$ given in Fig. 1 are used, with parabolic interpolation. The r.m.s. impulse response width of the fibre for a Lambertian quasimonochromatic source is shown in Figs. 2 and 3 by plain lines for three wavelengths of interest as a function of the exponent $\kappa$ in

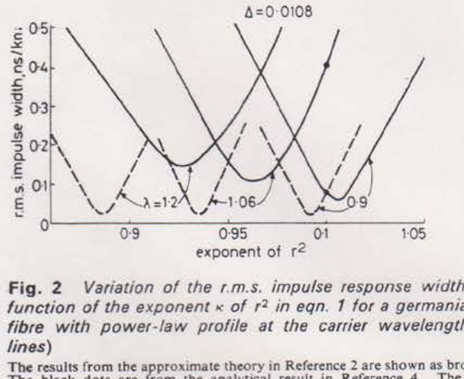


**Fig. 2** *Variation of the r.m.s. impulse response width $\sigma$ as a function of the exponent $\kappa$ of $r^2$ in eqn. 1 for a germania-doped fibre with power-law profile at the carrier wavelength (plain lines)*

The results from the approximate theory in Reference 2 are shown as broken lines. The black dots are from the analytical result in Reference 4. The germania concentration is assumed to be 10 mole % on axis and zero at the cladding. (Note that the impulse response is independent of the core radius.)





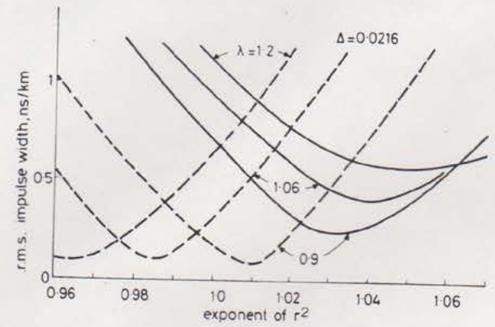


**Fig. 3** *Continuation of Fig. 1 for 20 mole % germania concentration on axis*

The approximate result from Reference 2 (interrupted lines) is, in that case, essentially unrelated to the exact result (plain lines)

eqn. 1. For comparison, the r.m.s. impulse response widths calculated from Reference 2 are shown by interrupted lines. As one can see, there are large discrepancies between the result obtained from the theory in Reference 2 and the exact result, particularly when $\lambda > 0{\cdot}9\mu m$ and $\Delta > 0{\cdot}01$. For example, when $\lambda = 1{\cdot}2\mu m$ and $\Delta = 0{\cdot}0216$, the simplified analytical formula in Reference 2 predicts that the minimum value of $\sigma$ is 0·08 ns/km when the exponent $\kappa$ is equal to 0·965. For that value of $\kappa$, $\sigma$ is, in fact, equal to 2 ns/km. The minimum value of $\sigma$ is obtained for $\kappa = 1{\cdot}05$ and is equal to 0·6 ns/km. The analytical formula presented in Reference 4, in contradistinction, can handle arbitrary variations of $n\,dn/d\lambda$ as a function of $n^2$. However, it is restricted to small departures of the profile from a square-law. For $\kappa = 1$ (square-law medium) our analytical result in Reference 4, shown by black dots in Figs. 2 and 3, agrees with the numerical result to better than three decimal places.

The determination of the optimum profile for a given class of material has been made, using our numerical technique, by successive approximations. For example, for a fibre with 13·5 mole % germania on axis ($\Delta = 0{\cdot}014$) and $\lambda = 1{\cdot}06\mu m$, we find that the r.m.s. impulse response width can be reduced to 52 ps/km by a proper selection of the coefficients of the expansion of $n^2(r)$ in series of $r^2$. This near-optimum profile departs very significantly from a power-law profile. The departure of the optimum profile from a power-law profile is found to be even more pronounced when two dopant materials such as boron oxide and germania, are used.

In conclusion, we have shown that, to evaluate the r.m.s. impulse response width of a multimode fibre it is essential to measure the variation of $dn/d\lambda$ as a function of $n$ at the carrier wavelength, as well as the profile $n(r)$ of the fibre, and to use a theory that takes the actual variation of $dn/d\lambda$ into account. The transmission rate capacity of fibres with $\Delta$ as large as 0·02 appears to be in the gigabit/s range, but the index profiles that one must look for are not, in general, power-law profiles.*

*Acknowledgments:* One of the authors (J.A.A.) expresses his thanks to E. A. J. Marcatili for useful discussions.

J. A. ARNAUD

*Bell Laboratories*
*Crawford Hill Laboratory*
*Holmdel, N.J. 07733, USA*

J. W. FLEMING

*Bell Laboratories*
*Murray Hill, N.J. 07974, USA*

*8th March 1976*

### References

1 COHEN, L. G., KAISER, P., and MACCHESNEY, J. B., O'CONNOR, P. B., and PRESBY, H. M.: 'Transmission properties of a low-loss near-parabolic-index fiber', *Appl. Phys. Lett.*, 1975, **26**, p. 472
2 OLSHANSKY, R., and KECK, D. B.: 'Material effects on minimizing pulse broadening'. Topical Meeting on Optical Fibre Transmission, Williamsburg, Virginia, Jan. 1975, *Appl. Opt.*, 1976, **15**, p. 483
3 FLEMING, J. W.: 'Measurements of dispersion in $GeO_2$–$B_2O_3$ $SiO_2$ glasses'. Fall Meeting of the American Ceramic Society, Pocono Manor (Penn.) Oct. 1975
4 ARNAUD, J. A.: 'Pulse broadening in multimode graded-index fibers', *Electron. Lett.*, 1975, **11**, pp. 8–9

* Note that, in real fibres, the profile is likely to fluctuate slowly and randomly about the optimum profile. This fluctuation causes the pulse width to increase as the square-root of the fibre length rather than in proportion of the fibre length, an effect unrelated to mode coupling

## PRODUCTION AND PROPERTIES OF $Al_2O_3$ LAYERS ON SILICON SUBSTRATES

*Indexing terms: Aluminium compounds, Insulating thin films, Metal-insulator-semiconductor structures*

A method for preparation of thin $Al_2O_3$ films using pyrolytic reactions is proposed and some electrical and optical properties of the films are investigated. The applicability of the films as an active dielectric in m.o.s. structures is discussed.

Thermal oxidation of silicon is usually used for production of oxides in m.o.s. structures. This oxide is characterised with a relatively low value of the built-in charge, low density of the electron states on the interface and high resistivity. However, a redistribution of the impurities in the silicon occurs during the production of oxide with such properties.[1] Besides, $SiO_2$ is characterised by a low dielectric constant and a high mobility of the alkaline ions, usually Na which leads to instabilities of the devices. For this reason, technologies for low temperature production of dielectrics with a high dielectric constant and resistant against the migration of mobile ions are needed. Such dielectrics can be successively used in production of semiconductor devices not only on Si substrates but also on other semiconductor substrates which cannot be thermally oxidised, for example GaAs. It is known that $Al_2O_3$ is a dielectric which satisfies these requirements to a large extent. For its production mainly low temperature vacuum methods[2, 3] and pyrolytic reactions are used.[4, 5]

The present paper presents a method for production of thin $Al_2O_3$ films and investigation of their properties as an active dielectric in m.o.s. structures.

According to this method the deposition rate of the layers can be from 10 to 100 Å/s. The layers are smooth without polycrystalline structure when observed under a microscope with 480 × magnification.

The $Al_2O_3$ layers are obtained on Si substrate at temperatures 750°–850°C in hydrogen atmosphere with $1 \times 10^{-2} - 5 \times 10^{-2}$ HCl and $1 \times 10^{-4} - 3 \times 10^{-4}$ $H_2O$ molar concentration according to the reaction

$$2\,AlCl_3 + 3\,H_2O = Al_2O_3 + 6\,HCl.$$

Previously the substrates are etched in the same gas atmo-

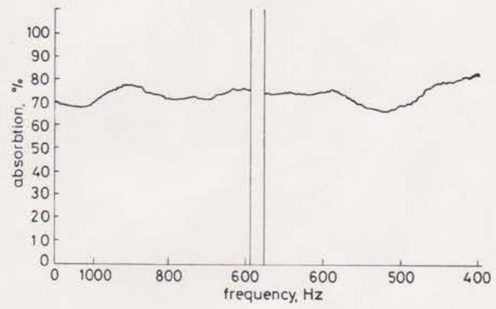


**Fig. 1** *I.R. absorption spectrum of the films*